Characterization of K-Complexes and Slow Wave Activity in a Neural Mass Model

Arne Weigenand[1,2] ◑, **Michael Schellenberger Costa[1,3]** ◑*, **Hong-Viet Victor Ngo[1,2,3]**, **Jens Christian Claussen[1,4]¶, Thomas Martinetz[1,2]¶**

1 Institute for Neuro- and Bioinformatics, University of Lübeck, Lübeck, Germany, **2** Graduate School for Computing in Medicine and Life Science, University of Lübeck, Lübeck, Germany, **3** Institute for Medical Psychology and Behavioral Neurobiology, University of Tübingen, Tübingen, Germany, **4** Computational Systems Biology, Jacobs University Bremen, Bremen, Germany

Abstract

NREM sleep is characterized by two hallmarks, namely K-complexes (KCs) during sleep stage N2 and cortical slow oscillations (SOs) during sleep stage N3. While the underlying dynamics on the neuronal level is well known and can be easily measured, the resulting behavior on the macroscopic population level remains unclear. On the basis of an extended neural mass model of the cortex, we suggest a new interpretation of the mechanisms responsible for the generation of KCs and SOs. As the cortex transitions from wake to deep sleep, in our model it approaches an oscillatory regime via a Hopf bifurcation. Importantly, there is a canard phenomenon arising from a homoclinic bifurcation, whose orbit determines the shape of large amplitude SOs. A KC corresponds to a single excursion along the homoclinic orbit, while SOs are noise-driven oscillations around a stable focus. The model generates both time series and spectra that strikingly resemble real electroencephalogram data and points out possible differences between the different stages of natural sleep.

Introduction

Several studies indicate a major role of slow wave sleep (SWS) in the consolidation of memories [1,2]. Especially its hallmarks, cortical slow oscillations (SO), are hypothesized to be a key mechanism for the transfer of memory into the neocortical long-term storage [3,4]. Furthermore, it has been shown that the efficacy of memory consolidation can be improved with oscillatory transcranial electric and phase-locked auditory stimulation [5–7].

In the human electroencephalogram (EEG) SOs are defined as waves with a frequency of 0.5–2 Hz and a peak-to-peak amplitude >75 μV [8,9]. Underlying the SO is a widespread, almost synchronous alternation of neocortical networks between phases of depolarization (active or up state) and hyperpolarization (silent or down state) [10,11], that behaves like a traveling wave [9,12]. Modeling and experimental studies indicate a role for both, synaptic mechanisms and intrinsic currents, in the generation of SOs [13–16].

The K-complex (KC) occurs at the pace of the SO [17] and is believed to be the EEG expression of the cellular slow oscillatory activity [18]. The negative peak of the KC marks the transition to the cellular up state [19]. A KC during light NREM sleep (N2) was identified to be an isolated down state [20]. Furthermore, KCs

show a high variability in morphology and amplitude, but are generally characterized as a negativepositive event with a sharp negative peak. Common variations of this theme are multiple peaks in the negative component or an initial positive bump before the negative-positive complex.

The components of evoked KCs were found to have typical latencies, namely the P200, N550 and P900 peaks. It was suggested that these components are not independent and share a common generation mechanism. Sometimes later components (N1500, P1900) with smaller amplitude are reported too [21,22].

The complexity of the brain on the structural as well as the neuronal level has, however, been challenging for theoretical studies and modeling approaches. Neural mass models, pioneered by the work of [23] and [24], successfully described many phenomena of the human EEG, e.g. alpha and gamma rhythms, evoked responses and epilepsy [25–27]. See [28] and [29] for reviews.

In addition to states of wakefulness sleep has been modeled within the neural mass framework, too. A parameter study by [30] revealed the importance of synaptic gains for the dominant frequency of neural mass models. Steyn-Ross et al. [31] investigated the effect of changes in the efficacy of excitatory connections and the resting membrane voltage, finding multiple stable states which they classified as sleep and wake.

Author Summary

In recent years, sleep has drawn increasing attention due to its multifunctional role, e.g. the involvement in the consolidation of memory. While neural mass models have been successfully employed to describe the dynamics of the awake brain, the drastic changes that arise during sleep have been challenging. As intracellular recordings point to a bistability in the membrane voltage of individual neurons, previous studies assumed a bistability to be responsible for the generation of SOs as well as KCs on the macroscopic scale. Here we present a minimal neural mass model of the cortex that we extend by a slow firing rate adaptation, which is assumed to underlie the termination of the cortical up state. A bifurcation analysis reveals the existence of a Hopf bifurcation together with an canard phenomenon. We show that these additional bifurcations are able to generate KCs as well as SOs, and reproduce the electroencephalogram (EEG) of sleeps stages N2 and N3 to a high degree. Based on these findings, we propose a new route for the sleep/wake transition, that is also consistent with the effect of neuromodulators on the brain.

While those features are generated within a -local- column of neural tissue, spatial components have been shown to lead to complex interactions with the intrinsic dynamics, e.g. Turing patterns and traveling waves [32,33]. However, within this study we focus on the generation of KCs as well as SOs rather than their spatial propagation. Nevertheless, our model can form the basis of a network of neural masses that covers spatial aspects, such as wave propagation.

Activity-dependent feedback via slow potassium channels has been suggested as a mechanism for the generation of SOs and KCs because of their sensitivity to the sleep related neuromodulator acetylcholine and their implication in the slow afterhyperpolarization [34,35]. Multiple studies also point out that potassium leak channels can be activated by several anesthetics [36–38]. In the neural mass framework additive and multiplicative adaptation mechanisms have been discussed by [39–41]. So far KCs were described as excursions from a stable silent state to an unstable active state and the related SOs as oscillations between those two states [42,43].

However, while for certain forms of anesthesia it seems plausible that the cortex undergoes a phase transition, it is not clear whether this necessarily holds for natural sleep [39,44]. Addressing these issues we present a neural mass model for the sleeping cortex which is extended by sodium dependent potassium current [45,46]. This approach links our neural mass model to modeling studies on SO generation based on single neurons as well as to experimental studies [14,16]. The model output resembles EEG time series of sleep stages N2 and N3 to a high degree and shows key features of spontaneous and evoked KCs.

Building upon a bifurcation analysis, we characterize the dynamic repertoire of the cortex model. Our analysis indicates that cortical SOs and KCs are related but different phenomena. We suggest a route for the transition from wake to deep sleep and point out differences between natural sleep and anesthesia.

Methods

In the following sections, we motivate and describe the mathematical foundation of the model. First, we introduce the concept of neural mass models and define the basic neural module we use as a starting point. Into this basic neural module, we incorporate a physiological plausible firing rate adaptation, characteristic for the sleeping cortex.

Neural mass framework

Instead of considering single neurons individually, an averaged representation of the respective neuron type describes the behavior of a whole population. The mean membrane voltage V_k of the neural population k is transformed into a firing rate Q_k via a sigmoidal mapping [25,47].

$$Q_k(V_k) = \frac{Q_k^{max}}{1 + \exp(-C(V_k - \theta_k)/\sigma_k)}. \tag{1}$$

Here, Q_k^{max} is the maximal firing rate of the respective population, while θ_k represents the firing threshold of the population and $1/\sigma_k$ the gain or steepness of the transition. $C = \pi/\sqrt{3}$ acts as a scaling factor that links the gain directly to the standard deviation of the change in firing rate dQ_k/dV_k.

At the dendrites, incoming spikes elicit transmitter release leading to the opening of synaptic channels. At any time, the fraction of open channels s_{mk} of type m at population k can be described by a convolution with an alpha function α_m [48], with

$$s_{mk} = \sum_{k'} \alpha_m N_{k'k} \otimes Q_{k'},$$
$$\alpha_m = \gamma_m^2 \, t \, \exp(-\gamma_m t). \tag{2}$$

Here, the inverse rise time γ_m determines its shape. The sum is over all spikes from different sources k' that arrive at the same type m of synapses at population k. We consider AMPAergic synapses for excitation and a generic GABAergic type for inhibition, leading to the second order differential equations

$$\begin{aligned}\ddot{s}_{ek} &= \gamma_e^2(N_{ek}Q_e(V_e) + \phi_n - s_{ek}) - 2\gamma_e \dot{s}_{ek}, \\ \ddot{s}_{ik} &= \gamma_i^2(N_{ik}Q_i(V_i) \quad - s_{ik}) - 2\gamma_i \dot{s}_{ik}.\end{aligned} \tag{3}$$

Here, $N_{k'k}$ stands for the mean number of synaptic connections of type k' to population k. While inhibitory populations only spread locally, there are two different sources of excitation: local inputs $N_{ek}Q_e(V_e)$ and background noise coming from unspecified brain structures ϕ_n, which is taken as uncorrelated Gaussian white noise with zero mean. To model external stimulation the mean of the background noise is elevated by ϕ_{stim} representing increased incoming spike rates.

The connectivity structure of our model is given in Figure 1. It consists of an excitatory and an inhibitory population coupled all to all.

An important assumption of most neural mass models is the existence of an equilibrium state V_0 the system is always close to [23]. However, this is not true for KCs and SOs and the scaling of synaptic currents with respect to the membrane voltage V_k becomes important. This was addressed by [49] with the introduction of a weighting term $(V_k - E_{rev})$.

Their model can be written similar to the classical conductance based form of [50] with one leak and two synaptic currents as
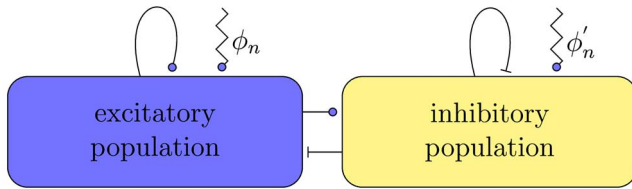
Figure 1. Connectivity of the cortex. The two populations are all to all coupled. In addition to intrinsic activity both populations receive background noise from unspecified brain structures. Circles indicate excitatory synapses, butts inhibitory synapses.
doi:10.1371/journal.pcbi.1003923.g001

$$\tau_k \dot{V}_k = -g_L(V_k - E_k^{rest})$$
$$-g_{AMPA}s_{ek}(V_k - E_{AMPA})$$
$$-g_{GABA}s_{ik}(V_k - E_{GABA}),$$
$$= -I_L - I_{AMPA} - I_{GABA}. \tag{4}$$

Here, g depicts the maximal conductivity, and E corresponds to the Nernst potentials of the respective channel.

The potential fluctuations measured in an EEG are mainly generated by pyramidal neurons [51]. Therefore, we use the membrane voltage of the excitatory population as our output variable. Similarly, multiple studies [25,49,52–54] used either the deviation of the membrane voltage from the resting state, $V_e - V_{rest}$, or the membrane voltage itself. As our system has no spatial extension and we only assume ohmic effects of skull and scalp, the EEG signal can be approximated by a linear scaling of the excitatory membrane voltage. When comparing experimental data and model output both time series are z-scored, because this linear transformation normalizes mean and standard deviation but preserves the other statistical properties of a signal. As we are only interested in qualitative properties of the model, e.g. the ratio between medium amplitude background oscillations and large amplitude deflections during N2, the different sleep stages are z-scored independently. For quantitative statements the same measuring function must be used.

Model extension with respect to sleep

As motivated in the introduction, we add the sodium dependent potassium current

$$I_{KNa} = g_{KNa} \frac{0.37}{1 + \left(\frac{38.7}{[Na]}\right)^{3.5}} (V_e - E_K),$$
$$[\dot{Na}] = (\alpha_{Na} Q_e(V_e) - Na_{pump}([Na]))/\tau_{Na} \tag{5}$$

to the excitatory population, see Equation 4. The current is connected to the excitatory membrane voltage by a membrane capacity $C_m = 1\ \mu F/cm$. Sodium influx responsible for I_{KNa} activation results from spiking or I_{NaP} activation, for which a depolarization above -60 mV is sufficient. We do not explicitly model these mechanisms but combine their effects via the V_e-determined spike rate Q_e and regard α_{Na} as average sodium influx per spike. Sodium extrusion is due to an active pump [55], which is detailed in Text S1. For simplicity, we neglect synaptic depression and other candidate mechanisms for additive feedback, like calcium dependent potassium currents.

This approach is qualitatively different to changes in the firing rate function, as utilized by [39]. Gradually switching between two firing rates alters the overall shape of the sigmoid function in a multiplicative activity-dependent manner, whereas we employ an additive threshold modulation.

Computational methods

The model was implemented in C++ and run within MATLAB [56]. The stochastic differential equations were iterated using a stochastic Runge-Kutta method of 4th order [57] with a step size of 0.1 ms. Simulation length was chosen as 30 s with a 5 s onset to ensure a steady state. All settings were run multiple times to check for robustness. Full model equations and parameters are given in Text S1 and Table S1. Bifurcation analysis is done with XPPaut [58], and a script is provided in Text S2.

Results

In the following, we analyze the dynamic repertoire of the model and define multiple dynamic regimes. We stress that the bifurcation analysis is done in the *noise free deterministic* case.

However, noise is able to push the system into different regimes, if the parameters are chosen sufficiently close to the border. Therefore, the analysis provides the repertoire of *possible* modes, whereas the corresponding response to external stimuli is captured in a following section.

Based on that description we show that the model is able to reproduce KCs as well as SOs. Furthermore, the analysis suggests a distinction between KCs and SOs and provides some insights in the differences between natural sleep and anesthesia. We will finally present a comparison of the noisy simulation to human EEG data.
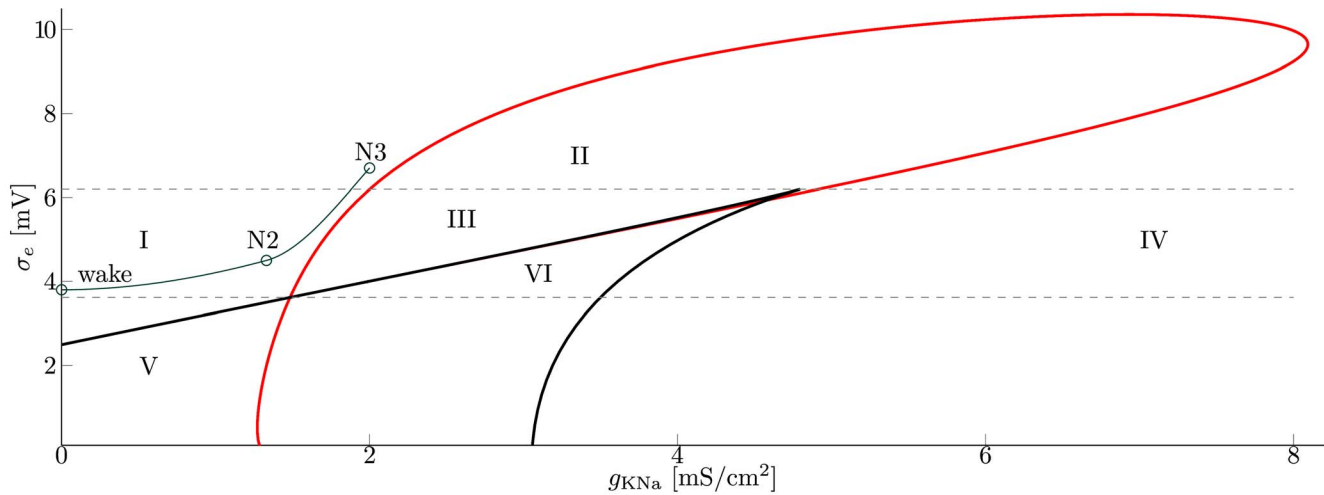
Bifurcation analysis

In order to characterize the dynamic repertoire of the cortical model we conducted a numerical bifurcation analysis of the noise-free system. The qualitative behavior of the model was most sensitive to changes in the inverse gain, σ_e, of the pyramidal population and the strength of the adaption, g_{KNa}.

Additionally, both parameters are known to be susceptible to changes in the neuromodulatory milieu, and the concentration of many major neuromodulators is known to change throughout the sleep-wake cycle. Cortical acetylcholine levels are lowest during slow wave sleep and highest during wake and REM sleep, whereas serotonin and norepinephrine levels are highest during wake, intermediate during SWS and lowest during REM sleep [59].

Tonic application of acetylcholine blocks leak and activity-dependent potassium currents I_{KLeak}, I_m, I_{KNa}, I_{KCa} (reviewed in [60]), as well as I_{NaP} [61]. Furthermore, many studies show that σ_e can be altered by norepinephrine, serotonin, acetylcholine as well as dopamine [35,62–69].

Consequently, σ_e and g_{KNa} were chosen as bifurcation parameters. The adaptation currents are primarily found in excitatory pyramidal cells and less so in inhibitory interneurons, which justifies the restriction of the parameter changes to the excitatory population.

As can be seen in Figure 2 the dynamics of the system is shaped by two bifurcations. The first one is a fold created by two saddle node bifurcations (black), that vanishes in a cusp. Between the two saddle nodes there are three equilibrium states, leading to bistability or excitability, see Figure 3a or Figure 3b. This is in good agreement with [31] and [70], as in the case of a fixed sodium concentration I_{KNa} is constant, and an increase in g_{KNa} acts as a decrease in resting potential.

Figure 2. Bifurcation diagram of the cortex with respect to g_{KNa} and σ_e. Overview over the models dynamic regimes, obtained via numerical bifurcation analysis of the cortex with respect to σ_e and g_{KNa}. Hopf bifurcations are drawn in red, while the black line depicts saddle-node bifurcations. The bottom gray line marks the intersection of Hopf and saddle curves, the top gray line the cusp bifurcation. The green line depicts the proposed route for the transition from wake to sleep stage N3. The region around wake corresponds to parameter settings commonly used for wake EEG. N2 and N3 are settings used within this study for the respective sleep stages, as given in Table 2 and 3. Regions I-VI are described in the text and Table 1 (Parameters as in Table S1).
doi:10.1371/journal.pcbi.1003923.g002

The second bifurcation is a Hopf arising at the upper stable branch (red). Importantly there is a canard explosion, where the small amplitude limit cycle of the Hopf bifurcation transitions into a high-amplitude relaxation cycle. This phenomenon was first described by [71] and is typical for systems where fast and slow subsystems interact. The relaxation cycle vanishes at the left saddle-node via a homoclinic bifurcation. At the cusp both saddle nodes coalesce and the homoclinic bifurcation turns into a second Hopf point.

Based on those bifurcations we define multiple dynamical regimes, see Table 1 for a short overview. Within region I a single stable state exists at depolarized membrane voltages where the cortex shows relatively high activity (see Figure 3). Especially for small values of g_{KNa} even large excitatory and inhibitory inputs only cause a passive response. A switch to the lower branch of the S-shaped curve in Figure 3 (region IV, silent state) is not possible.

Because of these properties we assume the waking brain to operate within this regime.

When crossing the curve of saddles to region V two new fixed points appear (see also Figure 3a). The system becomes bistable, with a stable active and silent state. Positive and negative inputs can cause a switching between the two stable branches.

A further increase in g_{KNa} turns the upper branch (active state) unstable. However, within region VI there are still multiple equilibria leaving the system excitable. Here a stimulus can produce a large positive response, which was previously thought to be responsible for the generation of KCs as well as SOs [72].

Only after the second saddle node is crossed the upper two equilibria vanish and a single stable state remains. This state is characterized by hyperpolarized membrane voltages leading to a quiescent cortex.
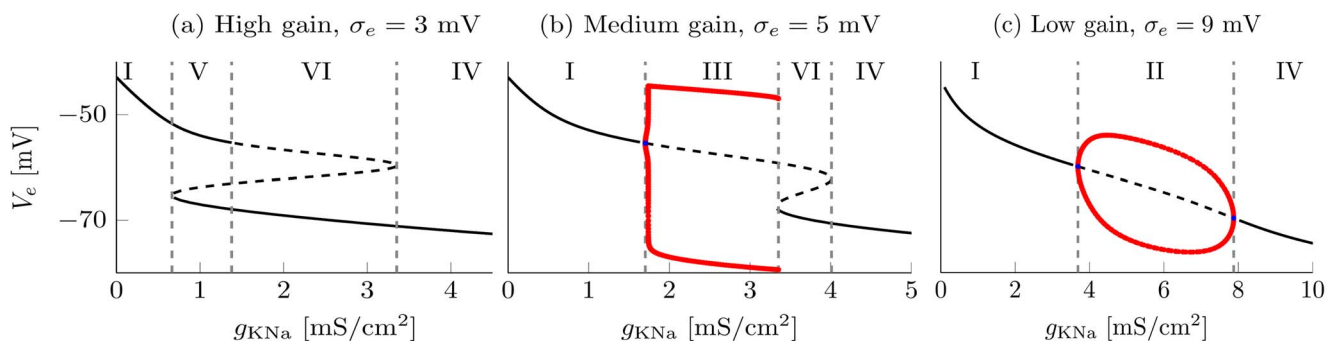
Figure 3. One-dimensional bifurcation diagrams for different gain levels σ_e. Low gain corresponds to high values of σ_e. Thick black lines depict stable fixed points, dashed lines unstable fixed points and red lines stable periodic solutions. The gray dashed lines mark bifurcations and separate the different regimes. (a) Two saddle-node bifurcations lead to excitability in region VI and bistability in region V. (b) A Hopf bifurcation appears (between I and III) in addition to the two saddle-nodes. The initial small amplitude limit cycle transitions into a high-amplitude relaxation cycle via a canard explosion. The high-amplitude periodic solutions vanish at the left saddle-node via a homoclinic bifurcation. The period of the relaxation oscillations goes to infinity as one approaches the homoclinic bifurcation. (c) Only the Hopf bifurcation remains, after the saddle nodes disappeared via a cusp bifurcation. Within region II there is no canard anymore.
doi:10.1371/journal.pcbi.1003923.g003

Table 1. Dynamic regimes of the cortical module.

Region	dynamical properties
I	active cortex
II	limit cycles
III	limit cycles and relaxation cycles
IV	silent cortex
V	bistable
VI	excitable

doi:10.1371/journal.pcbi.1003923.t001

Region III is characterized by periodic limit cycles or relaxation oscillations and, hence, high rhythmicity. The initial Hopf bifurcation is accompanied by a canard explosion: due to an exponentially small variation of the bifurcation parameter an abrupt transition from a medium-amplitude limit cycle to a high-amplitude relaxation cycle can take place.

This phenomenon was first described in [71] and is typical for systems where fast and slow subsystems interact. The corresponding one-dimensional bifurcation diagram is shown in Figure 3b. The periodic solutions vanish at the left saddle-node via a homoclinic bifurcation, and the period of the relaxation oscillations goes to infinity as one approaches the homoclinic bifurcation.

Additionally, with increasing σ_e the amplitude of the limit cycle increases and approaches the form of relaxation oscillations. This explains the similarity between the limit cycles and relaxation oscillations. Both are shaped by the same homoclinic orbit.

At the cusp the two saddle nodes vanish and the homoclinic bifurcation turns into a second Hopf point. Without the homoclinic bifurcation there is no canard anymore. Therefore, in region II above the cusp bifurcation only limit cycles remain, illustrated in Figure 3c, leading to high-amplitude oscillations.

Response to perturbations

While the bifurcation analysis provides the basic repertoire of the unperturbed model, its responsiveness with respect to perturbations, e.g. external stimuli or background noise, is crucial for its behavior. As mentioned before, within region I the cortex shows only a passive response. However, this changes for larger values of g_{KNa}, i.e. closer to the curve of Hopf points (red line in Figure 2, separating region I from II and III).

There, positive as well as negative inputs may cause a reverse spike resembling a KC. Additionally, close to the curve of Hopf points the stable active state turns into a stable focus, i.e. the system behaves like a damped oscillator upon perturbation. In Figure 4a we show the response to artificial stimuli ϕ_{stim} of varying strength, when the cortex is set close to the Hopf bifurcation between region I and III.

Stimuli of low strength lead to damped oscillations whose amplitudes are considerably larger than during the wake state but smaller than KCs or SOs. However, as the strength of the stimuli increases the system is pushed into the canard explosion and the amplitude of the response increases rapidly. While in Figure 4a there seems to be a threshold separating the two types of responses, it is actually a smooth transition given sufficiently small increases in stimulation strength.

The induced relaxation cycles show a good qualitative match with KCs seen during sleep. In the noise driven simulation the majority of inputs would lead to medium-amplitude oscillations, whereas only the rare outliers would trigger a KCs like response.
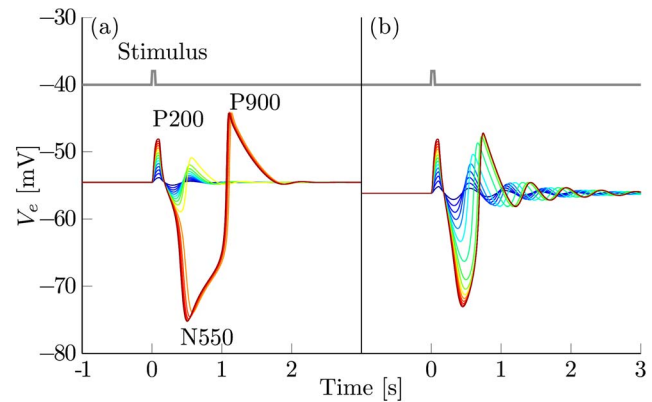
Figure 4. Response of the noise-free cortex to artificial stimuli. Excitatory bursts of 50 ms duration were applied to both populations. The spike rate of the stimuli ϕ_{stim} varies uniformly from 5 Hz (dark blue) to 100 Hz (dark red). The stimulus is shown in grey. (a) Bifurcation parameters are set to the mark N2 close to region III (see Table 2). There, a canard explosion leads to large amplitude responses that qualitatively resemble a typical evoked KC with its P200, N550 and P900 components. (b) Parameters are set to mark N3, so that the cortex is beyond the cusp close to region II (see Table 3). The canard vanished, leading to an even increase in the amplitude of the response.
doi:10.1371/journal.pcbi.1003923.g004

This is in good agreement with the dynamics seen in sleep stage N2, where medium-amplitude background oscillations are interrupted by large amplitude KCs.

We assume this mechanism to be responsible for the generation of KCs during sleep stage N2. Furthermore, this requires the cortex to be in the *active* state close to the Hopf bifurcation to region III, rather than being in the silent down state. This is in good agreement with multiple studies who report that during SWS of naturally sleeping animals more time is spent in up states than in down states [73–78].

Close to the Hopf, an increase of the inverse gain, σ_e, leads to an *increase* in the amplitude of the background oscillations and they approach the shape of a relaxation cycle. Beyond the cusp the canard vanishes and isolated events in the sense of KCs are not possible anymore (see Figure 4b).

This behavior is well reflected in what is seen during sleep stage N3, where SOs appear as large amplitude oscillations, that are *not* separated from the ongoing background activity. Furthermore, it explains the high similarity between KCs and SOs, as they are both shaped by the same homoclinic orbit. We hypothesize that during sleep stage N3 the cortex is in region I close to the Hopf bifurcation to region II.

Together these findings give rise to a new interpretation of the sleep/wake transition. At the transition to sleep stage N2, the cortex approaches the Hopf bifurcation close to region III, which shifts the EEG trace to higher amplitudes and lower frequencies compared to wake activity. By virtue of a canard explosion this background activity is then interrupted by single, isolated relaxation cycles. As sleep deepens further, the cortex follows the route depicted in Figure 2, while the amplitude of the background oscillations increases and ultimately approaches the form of a KC.

However, this is in contrast with the view that the cortex undergoes a phase transition when entering NREM sleep. Interestingly, a similar model was utilized to describe characteristics of anesthesia [39]. We can reproduce similar behavior, e.g. burst suppression in region VI (See Supplementary Figure S1).

Reproduction of sleep stages N2 and N3

To verify the ability of the model to reproduce sleep stage N2 we set the model to parameter configuration "N2" from Figure 2 (See Table 2). The chosen parameter set is within region I close to the border of region III, an example time series is shown in Figure 5.

In a region close to the chosen parameters the cortex is in the up state and shows the expected noise-driven medium-amplitude oscillations. In addition, background noise may push the model into high-amplitude deflections that closely resemble KCs seen in human EEG. Similar to the data the KCs can show a single pronounced peak or a prolonged down state, which depends on the noise.

Following our route for the sleep/wake transition in Figure 2 we then moved along the Hopf bifurcation to a setting beyond the cusp and close to region II, labeled as "N3". In Figure 6 a representative time series is shown with the parameters given in Table 3. There the cortex shows high amplitude oscillations around 0.8 Hz. In contrast to the N2 stage, the cortex does not produce KCs in the sense of isolated events that differ from the background oscillations. Rather, the response increases until it approaches the form of a KC, depending on the strength of the perturbation.

Discussion

Characterization of KCs and SOs

We explored an extended neural mass model of the cortex and related its multiple dynamical regimes to different sleep stages.

A bifurcation analysis revealed the existence of a fold as well as a Hopf bifurcation accompanied by a canard phenomenon. We argue that deflections generated by the canard explosion are identical to KCs seen in the EEG during natural sleep, leading to the spike-like nature of the KCs. Increasing the bifurcation parameter σ_e the canard vanishes, explaining the damped oscillatory behavior of SOs. Our analysis provides a clear theoretical distinction between KCs and SOs. However, as both the limit and the relaxation cycle are shaped by the same underlying homoclinic orbit, the actual transition is rather smooth even in the noise-free deterministic system (see Figure 4). Therefore, it might be challenging to find this distinction within experimental data.

Based on the bifurcation analysis we identified parameter regimes that show characteristics of sleep stage N2 and N3 and showed that our model is able to reproduce the EEG of both sleep stages to a high degree. Building upon these findings we propose an alternative scenario for the sleep wake transition. Rather than entering a bistable regime the cortex stays primarily within the active state. As sleep deepens, the cortex approaches the Hopf bifurcation, leading to an increase in amplitude and slowing of noise-driven background oscillations, as well as large amplitude deflections, i.e. KCs. At the transition to sleep stage N3 the canard phenomenon vanishes due to the cusp bifurcation. The remaining Hopf bifurcation is responsible for the generation of noise-driven SOs. Isolated events as in sleep stage N2 are not possible within that regime.

Parameter settings within region II or III lead to highly regular relaxation oscillations or limit cycles, that do *not* resemble human EEG. It is crucial that the cortex must be within region I *close* to region II or III to reproduce the data. In a study on resting state networks [79] found the awake brain to be in a state of criticality, which leads to an increased responsiveness. In this study, we also find the sleeping cortex close to a phase transition and suggest that the concept of criticality is not restricted to wakefulness, but carries over to sleep. However, the phase transition and computational goal are different.

Due to the presence of noise bifurcations do not lead to clear-cut qualitative changes of the dynamics [43]. Noise can shift critical points or induce behavior that is not seen in the deterministic case, such as noise-induced transitions.

Relation to intracellular recordings

Our work deals primarily with the characteristics of EEG signals during NREM sleep. However, the presented bifurcation analysis is useful in a broader context. Similar activity is found e.g. during non-REM sleep, anesthesia, coma and in isolated cortical preparations. It becomes increasingly clear that there exists a continuum of slow oscillatory states, which are mainly characterized by the fraction of time spent in up or down states, the temporal regularity with which state transitions occur and the response to external stimuli.

The phenomenon of up and down states in intracellular recordings is commonly associated with the notion of bistability or relaxation oscillations. However, it is important to note that most results on SOs were obtained in deeply anesthetized animals or slice preparations. Under these conditions, the system is down state dominated, i.e. down states last longer than up states, the occurrence of up states is often highly rhythmic [76,80] or up states are infrequent and transient [81]. In our model these classical regimes are also present, namely in regions III, V and VI.

Generally, SOs produced by anesthesia are much more regular than during natural sleep [76,82]. Under ketamine-xylazine anesthesia neurons spend twice the time in silent states compared to natural SWS [76], and in the auditory cortex of awake rats prolonged up states are not even observed at all [83]. Furthermore, SO properties differ from one anesthetic to the other [84]. Ketamine-xylazine anesthesia produces a uniform and continuous SO state [85], whereas with urethane epochs of stable SOs are short-lived and desynchronized periods may occur spontaneously [86]. This is similar to SWS where one finds waxing and waning of slow wave complexes interleaved with periods reminiscent of active states [74].

In contrast, [20] pointed out that a KC during light sleep is not always embedded in an ongoing SO, but is mostly an isolated event. Clearly, in N2 the active state dominates. Similarly, many studies report that during SWS of naturally sleeping animals more time is spent in up states than in down states [73–78] Furthermore, it has been reported that SWS contains many episodes of low-amplitude fast oscillations, lasting several seconds and resembling the active state [87]. This evidence points to natural sleep being up state dominated.

Table 2. Parameters of regime N2.

Symbol	Value	Unit	Description
σ_e	4.6	mV	inverse gain
g_{KNa}	1.33	mS/cm^2	conductivity

doi:10.1371/journal.pcbi.1003923.t002

(a)

(b)

5s
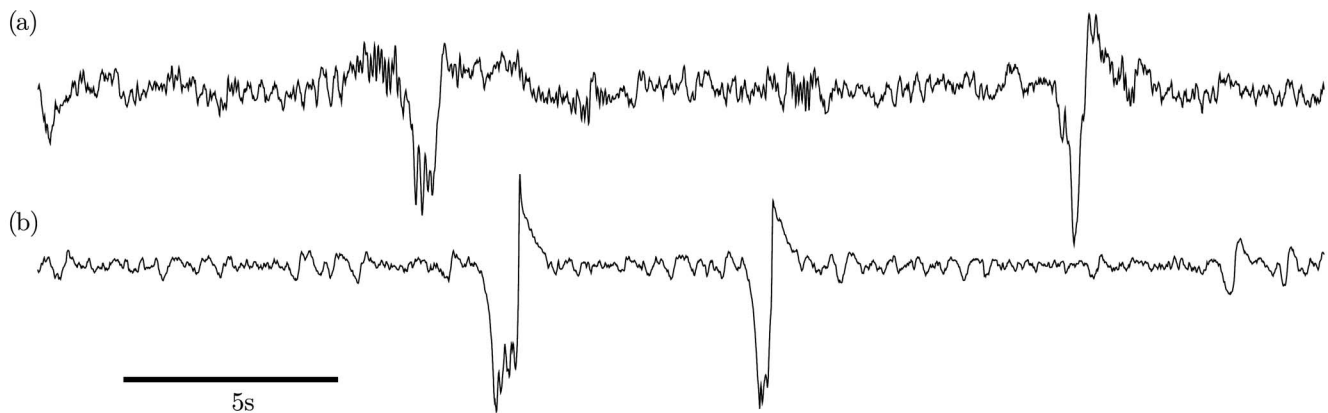
Figure 5. Comparison of human EEG with model output in regime N2. Qualitative comparison of (a) human EEG data of sleep stage N2 from electrode Cz with (b) the isolated cortical module in regime N2 (region IV in the bifurcation diagram in Figure 2). The traces illustrate the medium-amplitude background oscillations and the stereotypical shape of spontaneous KCs at the EEG level. It may or may not have an initial bump followed by a large negative peak and a pronounced positive overshoot. The model-KC is noise induced and represents a single relaxation cycle. An evoked KC in the noise-free case is shown in Figure 4a. Model output is excitatory membrane voltage V_e, and both time series are z-scored (Parameters as in Table 2).
doi:10.1371/journal.pcbi.1003923.g005

Furthermore, bistability is inferred via bimodality in the distribution of individual cells' membrane potential. In local field potentials, one can observe a markedly conserved waveform of individual SO events [88], but bimodality is already less visible. It is known that collective dynamics can exhibit, e.g. limit-cycle regimes, but at the same time emerge from irregular and high-dimensional neuronal activity, which is only apparent at small-scales [89].

The spectrum of SO phenomena cannot be fully captured by the concepts of bimodality or relaxation oscillations. Our analysis corroborates that the KC can be identified with a single, isolated relaxation cycle and slow wave activity, including prolonged episodes of low-amplitude fast oscillations, stems from noise-driven oscillations around a stable focus. Down states occur frequently in the up state dominated cortex, but they are transient.

Predictions

The assumption that a substantial gain change accompanies the change of sleep stages is reasonable, but still has to be clearly demonstrated experimentally for natural sleep. The only publication

we are aware of that touches this issue is [73]. Our model indicates that an increase in gain can induce a bistable state when awake, moving from region I to region V. Likewise, looking at comatose states (region IV) a decrease in gain should induce limit cycle oscillations.

Additionally, constant neural activation, i.e. arousal, causes relaxation oscillations in the model. Indeed, this phenomenon seems to occur in comatose patients, too, where one observes an increase in delta activity after stimulation [90]. This is termed paradoxical arousal and should not be confused with the paradoxical excitation/biphasic response during the induction process of anesthesia.

Furthermore, given the suggested role of gain change in the transition between N2 and N3, an altered slope of the f-I-relation of excitatory pyramidal cells could be a key factor in distinguishing wake and REM sleep.

Activity-dependent and leak potassium currents (or tonically activated extrasynaptic $GABA_A$ receptors) are both able to promote bistability in a cortical population. However, only activity-dependent mechanisms contribute to rhythmicity. It

(a)

(b)

5s
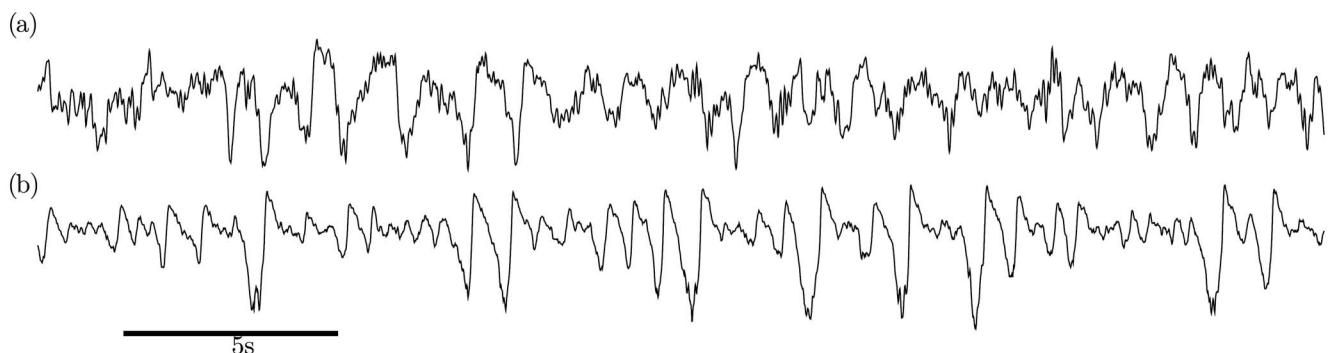
Figure 6. Comparison of human EEG with model output in regime N3. Qualitative comparison of (a) human EEG data of sleep stage N3 from electrode Cz with (b) the isolated cortical module in regime N3 (region I in the bifurcation diagram in Figure 2). As the system is close to the Hopf bifurcation noise leads to quasiperiodic oscillations around the stable focus (up state). Large amplitude oscillations resemble KCs as both are shaped by the same homoclinic orbit. The model output is excitatory membrane voltage V_e, and both time series are z-scored (Parameters as in Table 3).
doi:10.1371/journal.pcbi.1003923.g006

Table 3. Parameters of regime N3.

Symbol	Value	Unit	Description
σ_e	6.7	mV	inverse gain
g_{KNa}	2	mS/cm²	conductivity

would be interesting to see their contributions revealed for natural sleep and anesthesia.

A study by Molaee-Ardekani et al. [39] showed that a similar model of slow firing rate adaptation can reproduce the effects seen under anesthesia. A comparison of our findings with their results suggest that the region of bistability (V) as well as the region of excitability (VI) are actually associated with anesthesia.

Sleep: More than bistability and relaxation oscillations

A main result of this paper is that on the macroscopic level the cortex is not necessarily in a bistable regime during natural deep sleep. We argue that properties of KCs and SOs at the EEG level support the view of a monostable active cortex close to a Hopf and a saddle node bifurcation.

We stress that the characterization of KCs and SOs is made on the *population* level. While the switching between up and down states on the cellular level points to relaxation oscillations or bistability with noise-driven transitions, relatively regular oscillation at the cellular level may appear less regular at the EEG level, due to varying spatial synchrony [82]. Relaxation oscillations in the EEG usually correspond to pathological conditions like epilepsy.

We have not explicitly analyzed other adaptation mechanisms like multiplicative feedback arising due to synaptic depression or depletion of extra-cellular calcium or inhibitory modulation [91]. However, the additive activity-dependent feedback investigated here is sufficient to account for a multitude of phenomena in healthy and pathological conditions. Furthermore, we expect that the bifurcation structure of the system, i.e. presence of saddle-nodes, Hopf and homoclinic bifurcation, will persist in alternative settings. Thus, our main conclusions do not depend on the particular choice of the feedback mechanism.

Supporting Information

Figure S1 Burst suppression in region VI. Within region VI the system shows characteristics of burst suppression. A quiescent stable down state is interrupted by large amplitude excursions around the unstable active state.
(TIF)

Table S1 Parameters. Description and values of all parameters that are not subject of the bifurcation analysis.
(PDF)

Text S1 Full model equations. Full mathematical description of the model used within this study.
(PDF)

Text S2 Bifurcation analysis code. Script file used for the bifurcation analysis in XPPaut.
(PDF)

Video S1 Visualization of the sleep-wake transition. This video illustrates the change of the evoked response to perturbations, as the model follows the proposed sleep-wake transition depicted in Figure 2. Close to the "wake" state, the system immediately returns to the stable fixed point, without any oscillatory behavior. At the onset of sleep, g_{KNa} and σ_e increase and the system approaches the Hopf bifurcation, such that perturbations away from the active state lead to transient, small and slow oscillatory responses. However, as there are no large deflections, which resemble KCs this regime corresponds to sleep stage N1. Close to label "N2" in Figure 2, KCs emerge as isolated events through a canard explosion (Sleep stage N2). With further transition into deeper sleep, the amplitude of the background oscillations increases and approaches the relaxation cycle of the canard. Finally in the proximity of "N3" in Figure 2 there are no KCs in the sense of isolated events, but large amplitude slow oscillations around a stable focus (Sleep stage N3).
(MP4)

Acknowledgments

Author Contributions

Conceived and designed the experiments: AW MSC HVVN JCC TM. Performed the experiments: AW MSC. Analyzed the data: AW MSC HVVN. Wrote the paper: AW MSC HVVN JCC TM.

References

1. Walker MP, Stickgold R (2004) Sleep-dependent learning and memory consolidation. Neuron 44: 121–33.
2. Rasch B, Born J (2013) About sleep's role in memory. Physiol Rev 93: 681–766.
3. Rosanova M, Ulrich D (2005) Pattern-specific associative long-term potentiation induced by a sleep spindle-related spike train. The Journal of Neuroscience 25: 9398–9405.
4. Cox R, Hofman WF, Talamini LM (2012) Involvement of spindles in memory consolidation is slow wave sleep-specific. Learn Mem 19: 264–267.
5. Marshall L, Helgadóttir H, Mölle M, Born J (2006) Boosting slow oscillations during sleep potentiates memory. Nature 444: 610–613.
6. Antonenko D, Diekelmann S, Olsen C, Born J, Mölle M (2013) Napping to renew learning capacity: enhanced encoding after stimulation of sleep slow oscillations. Eur The Journal of Neuroscience 37: 1142–1151.
7. Ngo HVV, Martinetz T, Born J, Mölle M (2013) Auditory closed-loop stimulation of the sleep slow oscillation enhances memory. Neuron 78: 545–553.
8. Achermann P, Borbély AA (1997) Low-frequency (<1 Hz) oscillations in the human sleep electroencephalogram. Neuroscience 81: 213–222.
9. Steriade M (2003) The corticothalamic system in sleep. Frontiers in Bioscience 8: 878–899.
10. Massimini M, Huber R, Ferrarelli F, Hill S, Tononi G (2004) The sleep slow oscillation as a traveling wave. The Journal of Neuroscience 24: 6862–70.
11. Peyrache A, Dehghani N, Eskandar EN, Madsen JR, Anderson WS, et al. (2012) Spatiotemporal dynamics of neocortical excitation and inhibition during human sleep. Proceedings of the National Academy of Sciences of the United States of America 109: 1731–6.
12. Sanchez-Vives MV, McCormick DA (2000) Cellular and network mechanisms of rhythmic recurrent activity in neocortex. Nature Neuroscience 3: 1027–1034.
13. Bazhenov M, Timofeev I, Steriade M, Sejnowski TJ (2002) Model of thalamocortical slow-wave sleep oscillations and transitions to activated States. The Journal of Neuroscience 22: 8691–8704.
14. Compte A, Sanchez-Vives MV, McCormick DA, Wang XJ (2003) Cellular and network mechanisms of slow oscillatory activity (<1 Hz) and wave propagations in a cortical network model. Journal of Neurophysiology 89: 2707–2725.

15. Holcman D, Tsodyks M (2006) The emergence of Up and Down states in cortical networks. PLoS Computational Biology 2: e23.

16. Benita JM, Guillamon A, Deco G, Sanchez-Vives MV (2012) Synaptic depression and slow oscillatory activity in a biophysical network model of the cerebral cortex. Frontiers in Computational Neuroscience 6: 64.

17. Amzica F, Steriade M (1997) The K-complex: its slow (<1 Hz) rhythmicity and relation to delta waves. Neurology 49: 952–959.

18. Steriade M, Amzica F (1998) Slow sleep oscillation, rhythmic K-complexes, and their paroxysmal developments. Journal of Sleep Research 7 Suppl 1: 30–35.

19. Nir Y, Staba RJ, Andrillon T, Vyazovskiy VV, Cirelli C, et al. (2011) Regional Slow Waves and Spindles in Human Sleep. Neuron 70: 153–169.

20. Cash SS, Halgren E, Dehghani N, Rossetti AO, Thesen T, et al. (2009) The human K-complex represents an isolated cortical down-state. Science 324: 1084–1087.

21. Bastien CH, Crowley KE, Colrain IM (2002) Evoked potential components unique to non-REM sleep: relationship to evoked K-complexes and vertex sharp waves. International Journal of Psychophysiology 46: 257–274.

22. Colrain IM (2005) The K-complex: a 7-decade history. Sleep 28: 255–273.

23. Wilson HR, Cowan JD (1973) A mathematical theory of the functional dynamics of cortical and thalamic nervous tissue. Kybernetik 13: 55–80.

24. Lopes Da Silva FH, Hoeks A, Smits H, Zetterberg LH (1974) Model of brain rhythmic activity. The alpha-rhythm of the thalamus. Kybernetik 15: 27–37.

25. Jansen BH, Zouridakis G, Brandt ME (1993) A neurophysiologically-based mathematical model of flash visual evoked potentials. Biological Cybernetics 283: 275–283.

26. Wendling F, Bartolomei F, Bellanger JJ, Chauvel P (2002) Epileptic fast activity can be explained by a model of impaired GABAergic dendritic inhibition. Eur The Journal of Neuroscience 15: 1499–1508.

27. David O, Friston KJ (2003) A neural mass model for MEG/EEG:coupling and neuronal dynamics. NeuroImage 20: 1743–1755.

28. Coombes S (2005) Waves, bumps, and patterns in neural field theories. Biological cybernetics 93: 91–108.

29. Deco G, Jirsa VK, Robinson PA, Breakspear M, Friston K (2008) The dynamic brain: from spiking neurons to neural masses and cortical fields. PLoS Computational Biology 4: e1000092.

30. Robinson PA, Rennie CJ, Rowe DL (2002) Dynamics of large-scale brain activity in normal arousal states and epileptic seizures. Phys Rev E 65: 041924.

31. Steyn-Ross DA, Steyn-Ross ML, Sleigh JW, Wilson MT, Gillies IP, et al. (2005) The Sleep Cycle Modelled as a Cortical Phase Transition. The Journal of Biological Physics 31: 547–569.

32. Steyn-Ross ML, Steyn-Ross DA, Sleigh JW, Wilson MT (2011) A Mechanism for Ultra-Slow Oscillations in the Cortical Default Network. Bulletin of mathematical biology: 73: 398–416.

33. Steyn-Ross ML, Steyn-Ross DA, Sleigh JW (2013) Interacting Turing-Hopf Instabilities Drive Symmetry-Breaking Transitions in a Mean-Field Model of the Cortex: A Mechanism for the Slow Oscillation. Physical Review X 3: 021005.

34. Steriade M, Nuñez A, Amzica F (1993) A novel slow (<1 hz) oscillation of neocortical neurons in vivo: depolarizing and hyperpolarizing components. The Journal of Neuroscience 73: 3252–3265.

35. Hasselmo ME, Giocomo LM (2006) Cholinergic modulation of cortical function. Journal of Molecular Neuroscience 30: 133–135.

36. Patel AJ, Honoré E, Lesage F, Fink M, Romey G, et al. (1999) Inhalational anesthetics activate two-pore-domain background K+ channels. Nature Neuroscience 2: 422–426.

37. Nicoll RA, Malenka RC, Kauer JA (1990) Functional comparison of neurotransmitter receptor subtypes in mammalian central nervous system. Physiol Rev 70: 513–565.

38. Talley EM, Bayliss DA (2002) Modulation of TASK-1 (Kcnk3) and TASK-3 (Kcnk9) potassium channels volatile anesthetics and neurotransmitters share a molecular site of action. Journal Biological Chemistry 277: 17733–17742.

39. Molaee-Ardekani B, Senhadji L, Shamsollahi MB, Vosoughi-Vahdat B, Wodey E (2007) Brain activity modeling in general anesthesia: enhancing local mean-field models using a slow adaptive firing rate. Phys Rev E 76: 41911.

40. Loxley PN, Robinson PA (2007) Spike-rate adaptation and neuronal bursting in a mean-field model of brain activity. Biological Cybernetics 97: 113–122.

41. Ghorbani M, Mehta MR, Bruinsma R, Levine A (2012) Nonlinear-dynamics theory of up-down transitions in neocortical neural networks. Phys Rev E 85: 021908.

42. Wilson MT, Steyn-Ross DA, Sleigh JW, Steyn-Ross ML, Wilcocks L, et al. (2006) The K-complex and slow oscillation in terms of a mean-field cortical model. Journal of Computational Neuroscience 21: 243–257.

43. Curto C, Sakata S, Marguet S, Itskov V, Harris KD (2009) A simple model of cortical dynamics explains variability and state dependence of sensory responses in urethane-anesthetized auditory cortex. The Journal of Neuroscience 29: 10600–12.

44. Wilson MT, Barry M, Reynolds JNJ, Crump WP, Steyn-Ross AD, et al. (2010) An analysis of the transitions between down and up states of the cortical slow oscillation under urethane anaesthesia. Journal of Biological Physics 36: 245–259.

45. Schwindt PC, Spain WJ, Crill WE (1989) Long-lasting reduction of excitability by a sodium-dependent potassium current in cat neocortical neurons. Journal of Neurophysiology 61: 233–244.

46. Bischoff U, Vogel W, Safronov BV (1998) Na+-activated K+ channels in small dorsal root ganglion neurones of rat. The Journal of Physiology 510: 743–54.

47. Robinson PA, Rennie CJ, Wright J (1997) Propagation and stability of waves of electrical activity in the cerebral cortex. Phys Rev E 56: 826–840.

48. Tuckwell HC (1988) Introduction to theoretical neurobiology. Cambridge University Press.

49. Liley DTJ, Cadusch PJ, Wright J (1999) A continuum theory of electro-cortical activity. Neurocomputing 26–27: 795–800.

50. Hodgkin AL, Huxley AF, Katz B (1952) Currents carried by sodium and potassium ions through the membrane of the giant axon of Loligo. The Journal of Physiology 116: 424–448.

51. Buzsáki G, Anastassiou CA, Koch C (2012) The origin of extracellular fields and currents–EEG, ECoG, LFP and spikes. Nature Reviews Neuroscience 13: 407–420.

52. Steyn-Ross DA, Steyn-Ross ML, Wilcocks L, Sleigh JW (2001) Toward a theory of the general-anesthetic-induced phase transition of the cerebral cortex. II. Numerical simulations, spectral entropy, and correlation times. Physical Review E 64: 011918

53. Suffczyński P, Kalitzin S, Lopes Da Silva FH (2004) Dynamics of non-convulsive epileptic phenomena modeled by a bistable neuronal network. Neuroscience 126: 467–84.

54. Sotero RC, Trujillo-Barreto NJ (2008) Biophysical model for integrating neuronal activity, EEG, fMRI and metabolism. NeuroImage 39: 290–309.

55. Wang XJ, Liu Y, Sanchez-Vives MV, McCormick DA (2003) Adaptation and temporal decorrelation by single neurons in the primary visual cortex. Journal of Neurophysiology 89: 3279–3293.

56. MATLAB (2013). MATLAB:R2013b.

57. Küpper D, Kværnø A, Rößler A (2011) A Runge-Kutta method for index 1 stochastic differential-algebraic equations with scalar noise. BIT Numer Math 52: 437–455.

58. Ermentrout B (2003) Simulating, Analyzing, and Animating Dynamical Systems: A Guide to XPPAUT for Researchers and Students. SIAM Rev 45: 150–152.

59. Léna I, Parrot S, Deschaux O, Muffat-Joly S, Sauvinet V, et al. (2005) Variations in extracellular levels of dopamine, noradrenaline, glutamate, and aspartate across the sleep–wake cycle in the medial prefrontal cortex and nucleus accumbens of freely moving rats. Journal of Neuroscience Research 81: 891–9.

60. McCormick DA, Huguenard JR (1992) A model of the electrophysiological properties of thalamocortical relay neurons. Journal of Neurophysiology 68: 1384–400.

61. Mittmann T, Alzheimer C (1998) Muscarinic inhibition of persistent Na+ current in rat neocortical pyramidal neurons. Journal of Neurophysiology: 1579–1582.

62. Soma S, Shimegi S (2012) Cholinergic modulation of response gain in the primary visual cortex of the macaque. Journal of Neurophysiology: 283–291.

63. Disney AA, Aoki C, Hawken MJ (2007) Gain modulation by nicotine in macaque v1. Neuron: 701–713.

64. Polack PO, Friedman J, Golshani P (2013) Cellular mechanisms of brain state-dependent gain modulation in visual cortex. Nature Neuroscience 16: 1331–1339.

65. Timmons D, Geisert E, Stewart E, Lorenzon M, Foehring C (2004) Alpha 2 -Adrenergic receptor-mediated modulation of calcium current in neocortical pyramidal neurons. Brain Research 1014: 184–196.

66. Thurley K, Senn W, Lüscher H (2008) Dopamine increases the gain of the input-output response of rat prefrontal pyramidal neurons. Journal of Neurophysiology. 99: 2985

67. Zhang ZW, Arsenault D (2005) Gain modulation by serotonin in pyramidal neurones of the rat prefrontal cortex. The Journal of Physiology 2: 379–394.

68. Mehaffey WH, Doiron B (2005) Deterministic multiplicative gain control with active dendrites. The Journal of Neuroscience 25: 9968–9977.

69. Gulledge AT, Bucci D (2009) M1 receptors mediate cholinergic modulation of excitability in neocortical pyramidal neurons. The Journal of Neuroscience 29: 9888–9902.

70. Robinson PA, Phillips JK, Fulcher BD, Puckeridge M, Roberts JA (2011) Quantitative modelling of sleep dynamics. Philos Trans A Math Phys Eng Sci 369: 3840–3854.

71. Benoît E, Callot JL, Diener F, Diener M (1981) Chasse au canard. Collectanea Mathematica 31–32: 37–119.

72. Wilson MT, Steyn-Ross ML, Sleigh JW (2005) Predictions and simulations of cortical dynamics during natural sleep using a continuum approach. Phys Rev E 72: 51910.

73. Steriade M, Timofeev I, Grenier F (2001) Natural waking and sleep states: a view from inside neocortical neurons. Journal of Neurophysiology 85: 1969–1985.

74. Destexhe A, Contreras D, Steriade M (1999) Spatiotemporal analysis of local field potentials and unit discharges in cat cerebral cortex during natural wake and sleep states. The Journal of Neuroscience 19: 4595–4608.

75. Timofeev I, Grenier F, Steriade M (2001) Disfacilitation and active inhibition in the neocortex during the natural sleep-wake cycle: an intracellular study. Proceedings of the National Academy of Sciences of the United States of America 98: 1924–9.

76. Chauvette S, Crochet S, Volgushev M, Timofeev I (2011) Properties of slow oscillation during slow-wave sleep and anesthesia in cats. The Journal of Neuroscience 31: 1499815008.

77. Ji D, Wilson M (2006) Coordinated memory replay in the visual cortex and hippocampus during sleep. Nature neuroscience 10: 100–107.

78. Vyazovskiy V, Olcese U, Lazimy Y (2009) Cortical firing and sleep homeostasis. Neuron 63: 865–878.

79. Deco G, Jirsa VK (2012) Ongoing cortical activity at rest: criticality, multistability, and ghost attractors. The Journal of Neuroscience 32: 3366–3375.

80. Deco G, Martí D, Ledberg A (2009) Effective reduced diffusion-models: a data driven approach to the analysis of neuronal dynamics. PLoS Computational Biology 5: e1000587

81. Poskanzer KE, Yuste R (2011) Astrocytic regulation of cortical UP states. Proceedings of the National Academy of Sciences of the United States of America 108: 18453–8.

82. Amzica F, Steriade M (1998) Electrophysiological correlates of sleep delta waves. Electroencephalogr Clin Neurophysiol 107: 6983.

83. Hromadka T, Zador AM, DeWeese MR (2013) Up states are rare in awake auditory cortex. Journal of Neurophysiology 109: 1989–1995.

84. Amzica F, Steriade M (1997) Cellular substrates and laminar profile of sleep k-complex. Neuroscience 82: 671–686.

85. Ruiz-Mejias M, Ciria-Suarez L, Mattia M, Sanchez-Vives MV (2011) Slow and fast rhythms generated in the cerebral cortex of the anesthetized mouse. Journal of Neurophysiology 106: 2910–21.

86. Clement EA, Richard A, Thwaites M, Ailon J, Peters S, et al. (2008) Cyclic and sleep-like spontaneous alternations of brain state under urethane anaesthesia. PLoS ONE 3: e2004.

87. Destexhe A, Sejnowski TJ (2003) Interactions between membrane conductances underlying thalamocortical slow-wave oscillations. Physiological reviews 83: 1401–53.

88. Crunelli V, Hughes SW (2010) The slow (<1 Hz) rhythm of non-REM sleep: a dialogue between three cardinal oscillators. Nature neuroscience 13: 9–17.

89. Boustani SE, Destexhe A (2010) Brain dynamics at multiple scales: can one reconcile the apparent low-dimensional chaos of macroscopic variables with the seemingly stochastic behavior of single neurons? International Journal of Bifurcation and Chaos 20: 1687–1702.

90. Evans BM (1976) Patterns of arousal in comatose patients. Journal of Neurology, Neurosurgery, and Psychiatry 39: 392–402.

91. Sanchez-Vives MV, Mattia M, Compte A, Perez-Zabalza M, Winograd M, et al. (2010) Inhibitory modulation of cortical up states. Journal of Neurophysiology 104: 1314–24.